Self-Assembly and Autopolymerization of Pyrrole and Characteristics of Electrodeposition of Polypyrrole on Roughened Au(111) Modified by Underpotentially Deposited Copper

Yu-Chuan Liu*,† and Thomas C. Chuang‡

Department of Chemical Engineering, and Polymer Material R&D Center, Van Nung Institute of Technology, 1 Van Nung Road, Shuei-Wei Li, Chung-Li City, Tao-Yuan, Taiwan, Republic of China

Received: February 26, 2003; In Final Form: July 2, 2003

By combining techniques of underpotential deposition (UPD) and roughening metal substrates by a triangular-wave oxidation−reduction cycle (ORC) which is generally used in surface-enhanced Raman scattering (SERS) studies, and extending applications of self-assembled monolayers (SAMs), copper is underpotentially deposited on electrochemically roughened Au(111) in this study for the first time. The formation of SAMs and further autopolymerization of pyrrole monomers are found on the UPD Cu-modified gold surfaces. The stability of SAMs is significantly improved due to the presence of UPD Cu. Furthermore, electropolymerized polypyrrole (PPy) on this UPD Cu-modified roughened Au demonstrates some distinguishing properties. These include higher conductivities, higher intensity, and better resolution on SERS and improved anti-aging ability in a 50% relative humility, 20% (v/v) O_2 atmosphere at 30 °C for 60 days.

Introduction

Self-assembled monolayers (SAMs) can be formed by the spontaneous adsorption of organic molecules onto a metal or metal oxide surface, especially for alkanethiols adsorbing on copper, silver, and particularly gold.[1,2] The ease and flexibility of the self-assembly process provides a convenient method for altering the properties of the metal as an electrode.[3,4] On these metals, thiols and related molecules form a densely packed, oriented monolayer.[5,6] The assemblies are the product of strong metal−sulfur interactions that are also responsible for the robust nature of the SAM in liquid. Successful SAMs require a relatively strong bond between the substrate and an atom or moiety in the molecule, and an additional lateral interaction between molecules in the monolayer. Therefore, SAMs provide a facile means of defining the chemical composition and structure of a surface; they have been widely used in inhibiting metal corrosion[7] and promoting better adhesion of electroactive polymers.[8] In general, the lack of stability of these films during long-term exposure to the atmosphere or to higher temperatures results in some restrictions to their application.[9,10] Strategies to improve the stability of SAMs include achieving multiple gold/sulfur interactions[11] or incorporating polymerizable groups[12] or aromatic moieties.[13] A recent innovation was to form a single atomic layer of copper or silver on a gold surface by underpotential deposition (UPD) and to assemble a monolayer on the UPD layer.[14,15] There is growing evidence that the bond between the sulfur and the UPD atom is stronger than the bond between the sulfur and gold atoms, which results in more stable SAMs.

As is generally known, many UPD metals can form a monolayer on the foreign metal substrate at potentials positive from the onset of bulk reduction taking place; they display catalytic effects for various electrochemical reactions.[16,17] Zamborini et al.[14] reported the study of UPD Cu corrosion and passivation with SAMs of organomercaptan. A methyl-terminated aromatic SAM shifts the potential for UPD Cu oxidation more positive than a hydroxyl-terminated aromatic SAM. For longer chain *n*-alkanethiol SAMs, the presence of the UPD Cu layer markedly improves the stability of the SAM compared to that when it is adsorbed directly on the Au surface. Lin et al.[15] reported the study of SAMs of alkanoic acids on gold surfaces modified by UPD metals. The metal adlayers promote the anchoring of carboxylate headgroups and the assembly of ω-alkanoic acids, which would otherwise exhibit no chemisorption on bare gold. The binding scheme is different from SAMs of alkanethiols on gold and alkanoic acids on silver or copper surfaces. Also, measurements from X-ray photoelectron spectroscopy (XPS) suggest that Au/Ag(UPD) is not prone to oxidation in air, as reported by Jennings and Laibinis.[11]

Besides the UPD metals, the oxidation−reduction cycle (ORC) procedure generally used for roughening metal substrates on surface-enhanced Raman scattering (SERS) studies can also provide an easy and reliable way to modify the metal substrates.[18,19] As shown in the literature,[20,21] the technique of SERS depends critically on the presence of structural features of dimensions 10−100 nm. It is generally accepted that the enhancement of the Raman emission of molecules adsorbed on the metal surface has a double origin: electromagnetic (EM) enhancement[22,23] and chemical (CHEM) enhancement.[24,25] EM enhancement results from the enhancement of local electromagnetic fields at the surface of a metal, mainly confined to Ag, Au, and Cu, which can support surface plasma/optical conduction resonances. In contrast, CHEM enhancement is associated with a charge transfer between the metal and adsorbate at atomic-scale roughness features. The electrochemical ORC procedures for roughening substrates generally involve two different methods. One is a triangular-wave ORC,[26,27] and the other is a square-wave ORC.[28,29] For producing a controllable surface roughness and a homogeneous surface, the former has an advantage over the latter.[30,31]

As shown in the literature,[32,33] the polymerized SAMs with a terminal pyrrole exhibit increased stability toward thermal

* Corresponding author. Tel.: 886-3-4515811 ext. 540. Fax: 886-2-86638557. E-mail: liuyc@cc.vit.edu.tw.
† Department of Chemical Engineering.
‡ Polymer Material R&D Center.

10.1021/jp0344996 CCC: $25.00
Published on Web 08/15/2003

desorption and greater resistance to exchange with solution thiols. Furthermore, the chemical and physical properties of conducting polymers (CPs), such as discharging behavior,[34,35] adhesion to the electrode surface,[32,36] surface roughness, and conductivity,[37,38] can be significantly enhanced by depositing the CPs on an electrode surface which has been first modified with an appropriate thiol or disulfide SAMs. Since SAMs, UPD metals, and ORC roughening can be individually used to modify metal substrates, the combination of these methods and ideas would multiply the corresponding effects. In this study, Au (111) substrates, electrochemically roughened by a triangular-wave ORC in an aqueous solution, were modified by UPD Cu, which is original and has not been reported before. By extending the idea of SAMs, the characteristics of autopolymerization and electropolymerization of pyrrole on these UPD Cu-modified Au substrates were examined in detail.

Experimental Section

Chemical Reagents. Pyrrole (Py) was triply distilled until a colorless liquid was obtained and was then stored under nitrogen before use. H_2SO_4, $CuSO_4$, $LiClO_4$, and KCl were used as received without further purification. The reagents (p.a. grade) were purchased from Acros Organics. All the solutions were prepared using deionized 18 MΩ cm water.

Preparation of Roughened Au Substrates. All the electrochemical experiments were performed in a three-compartment cell at room temperature (22°C) and were controlled by a potentiostat (model PGSTAT30, Eco Chemie). A sheet of single-crystal Au(111) foil with bare surface area of 0.238 cm^2, a 2 × 2 cm^2 platinum sheet, and a silver−silver chloride (Ag/AgCl) were employed as the working, counter, and reference electrodes, respectively. Before the ORC treatment, the Au(111) electrode was mechanically polished (model Minimet 1000, Buehler) successively with 1 and 0.05 μm of alumina slurry to a mirror finish. The electrode was then cycled in a deoxygenated aqueous solution containing 0.1 N KCl from −0.28 to +1.22 V vs Ag/AgCl at 500 mV/s with 25 scans. The durations at the cathodic and anodic vertexes are 10 and 5 s, respectively. After the ORC treatment, the roughened Au electrode (called the unmodified Au substrate) was rinsed throughout with deionized water and finally dried in a vacuum-dryer, in the absence light, for 1 h at room temperature for subsequent use.

Preparation of UPD Cu-Modified Roughened Au Substrates. The cathodic deposition potentials of UPD Cu and bulk Cu deposited on the electrochemically roughened Au substrates, as prepared above, were obtained from cyclic voltammograms from −0.22 to +0.75 V vs Ag/AgCl at 20 mV/s in 1.0 mM $CuSO_4$ and 0.1 M H_2SO_4 aqueous solutions. The substrates were then cycled in this range at 20 mV/s until the UPD Cu and bulk Cu waves became well-defined. Finally, the scan was stopped at 0.030 V vs Ag/AgCl, which is just prior to the onset of bulk Cu deposition, as will be shown later. The prepared Au/UPD Cu substrate (called UPD Cu-modified Au substrate) was immediately emersed and rinsed throughout with deionized water, and finally dried in a vacuum-dryer, in the absence of light, for 1 h at room temperature for subsequent use.

Autopolymerization and Electropolymerization of Pyrrole on the UPD Cu-Modified Au Substrates. A deoxygenated aqueous solution containing 0.5 M pyrrole was instantly dropped onto the as-prepared UPD Cu-modified Au substrate. It was then placed in a desiccator with nitrogen, in the absence of light, for 2 h. Finally, the sample (called autopolymerized PPy) was rinsed throughout with deionized water and dried in a vacuum-dryer, in the absence of light, at room temperature before the test. The electrochemical polymerization of PPy on UPD Cu-modified Au substrate (called electropolymerized PPy) was carried out at a constant anodic potential of 0.85 V vs Ag/AgCl in a deoxygenated aqueous solution containing 0.1 M pyrrole and 0.1 M $LiClO_4$. Before electropolymerization, it is necessary to wait ca. 15 min for reaching a steady value of the open-circuit potential (OCP). The charge passed was 5000, 25, and 25 mC cm^{-2} for conductivity, SERS, and X-ray photoelectron spectroscopy (XPS) measurements, respectively. For comparison, PPy was also electrodeposited on the unmodified Au substrate by using the same preparation conditions.

Characteristics of UPD Cu-Modified Au Substrates and Prepared PPy Films. The surface morphologies of the UPD Cu-modified Au substrate and the unmodified Au substrate were obtained using scanning electron microscopy (SEM, model S-4700, Hitachi). Raman spectra were obtained using an XY modular laser Raman spectrometer (Dior) employing a He−Ne laser of 1 mW radiating on the sample operating at 632.8 nm and a charge-coupled device (CCD) detector with 1 cm^{-1} resolution. For the XPS measurements, a Physical Electronics PHI 1600 spectrometer with monochromatized Mg Kα radiation, 15 kV and 250 W, and an energy resolution of 0.1−0.8% $\Delta E/E$ was used. To compensate for surface charging effects, all XPS spectra are referred to the C 1s neutral carbon peak at 284.6 eV. The complex XPS and SERS peaks are deconvoluted into component Gaussian peaks using peak separation and analysis software (PeakFit v4.0, AISN Software Inc.). In the XPS N 1s deconvolution, the four component peaks are located at ca. 398.2, 399.9 eV, and at higher than 401 eV of 401.7 and 402.8 eV with equal value of half-width at half-maximum (HWHM).

Before conductivity measurements, the PPy-based films were stripped from the electrodes with clear adhesive tape. They had a mechanical stability that made them well suited for the measurements. The conductivities of the PPy films were determined by using a four-probe technique with a direct current (dc) measurement at room temperature.[39] The conductivity value of the insulating tape without PPy film is ca. 1.1×10^{-7} S cm^{-1}, which has no influence on the measurement of the conductivity of the PPy film. The aging test was performed in an atmosphere of 50% relative humidity (RH) and 20% volume concentration (v/v) of O_2 in a mixture of O_2 and N_2 at 30 °C for 60 days.

Results and Discussion

Characteristics of UPD Cu-Modified Au Substrates. In an ORC treatment, the chloride electrolyte was selected; this facilitates the metal dissolution−deposition process that is known to produce SERS-active roughened surfaces.[40] Figure 1a shows the typical triangular voltammetry curve obtained at 500 mV s^{-1} on gold in 0.1 N KCl. As shown in previous studies,[41,42] Au- and Cl-containing nanocomplexes with microstructures smaller than 100 nm were formed on the roughened Au substrates after an ORC treatment. These formed nanocomplexes were stable because no anodic stripping was observed in 0.1 M H_2SO_4, as demonstrated in Figure 1b. Consequently, no dissolution of these nanocomplexes occurred for the subsequent deposition of UPD Cu on the roughened Au in 1.0 mM $CuSO_4$ and 0.1 M H_2SO_4. Figure 2a shows the typical voltammetric curve obtained at 20 mV s^{-1} on electrochemically roughened gold in 1.0 mM $CuSO_4$ and 0.1 M H_2SO_4. Figure 2b, obtained in 0.1 M H_2SO_4, is demonstrated as a reference. Comparing curves a and b of Figure 2, it is clear that the cathodic waves centered at 0.13 and −0.041 V vs Ag/AgCl correspond to the UPD and bulk depositions of Cu, respectively, which can be further confirmed from the deposition time-

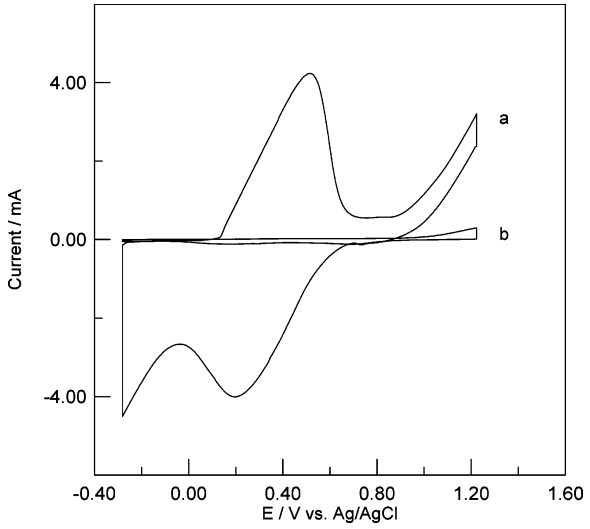

Figure 1. Cyclic voltammograms at 500 mV/s of the 25th scan for gold electrodes in different electrolytes: (a) in 0.1 N KCl and (b) in 0.1 N H_2SO_4.

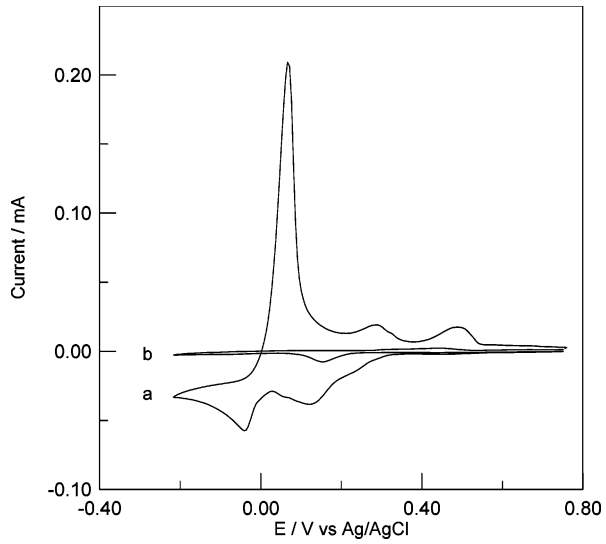

Figure 2. Cyclic voltammograms at 20 mV/s of the first scan for electrochemically roughened gold electrodes in different electrolytes: (a) in 1.0 mM $CuSO_4$ and 0.1 M H_2SO_4 and (b) in 0.1 M H_2SO_4.

resolved characteristic curves for UPD Cu and bulk Cu, as shown in Figure 3. Because only a monolayer or submonolayer of adatoms is deposited at the UPD potential, a typical charge passed−time plot, as illustrated in Figure 3a, is reasonably exhibited. The UPD deposition ceases when the formation of the monolayer is completed. At the end of deposition, the charge used is ca. 2260 μC/cm^2, which is ca. 5-fold the magnitude of the reported value of 445 μC/cm^2 for UPD Cu deposited on flat Au. In contrast, the bulk deposition of Cu on already deposited Cu is arbitrary. The deposition would proceed until there is a diffusion-controlled problem, as shown in Figure 3b.

The existence of UPD Cu on Au can be confirmed from the XPS analyses. Figure 4 a and b shows the XPS Cu $2p_{3/2-1/2}$ core-level spectra of UPD Cu and bulk Cu deposited on electrochemically roughened Au substrates, respectively. The bulk Cu was prepared by using a deposition procedure similar to that performed on the UPD Cu, as described in the Experimental Section, but the scan was stopped at the cathodic vertex of −0.22 V vs Ag/AgCl, at which the deposition of bulk Cu is just completed, as shown in Figure 2a. As reported by Zamborini et al.,[14] the XPS results of Cu(0) or Cu(I) cannot be

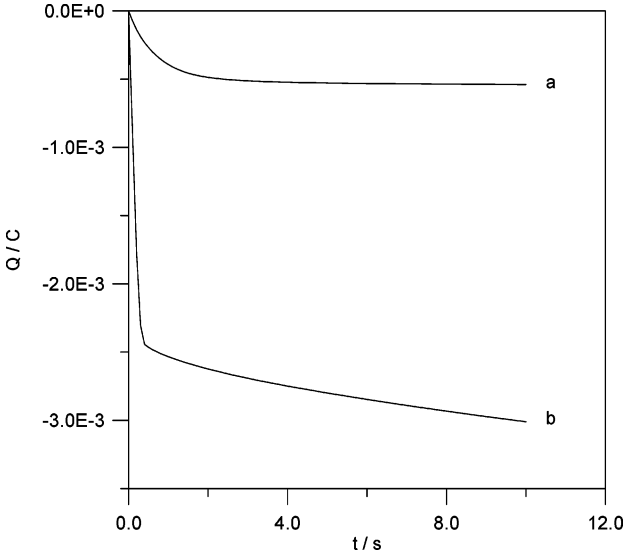

Figure 3. Coulometric curves of UPD Cu (a) and bulk Cu (b) deposited on electrochemically roughened gold substrates at cathodic potentials of 0.13 and −0.041 V vs Ag/AgCl, respectively.

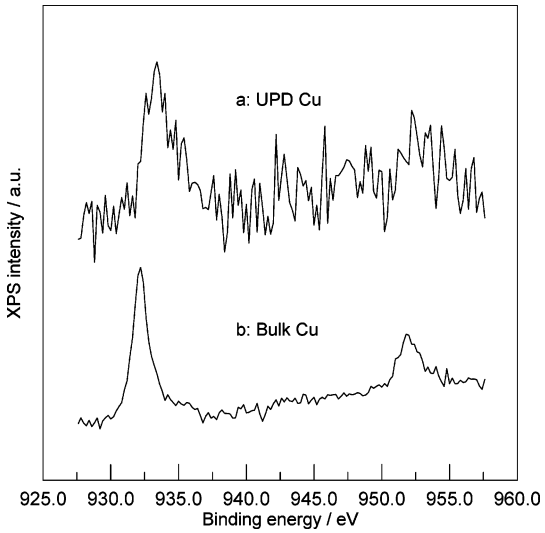

Figure 4. XPS Cu $2p_{3/2-1/2}$ core-level spectra of different coppers deposited on electrochemically roughened gold substrates: (a) UPD Cu and (b) bulk Cu.

distinguished between these two possibilities for UPD Cu deposited on flat Au. However, comparing spectra a and b of Figure 4, the Cu $2p_{3/2}$ main peak of the UPD Cu is located at 933.4 eV with a positive shift of 1.2 eV with respect to that of bulk Cu. XPS analysis of our previous study of UPD Cu on PPy[44] and UPD Cu on Pt reported in the literature[45] also show positive shifts of 0.50 and 0.95 eV with respect to those of bulk Cu, respectively. Clearly, the UPD Cu deposited on electrochemically roughened Au in this study is well-defined. It appears as a type of positively charged Cu which is distinguished from the bulk Cu with zero charge.

Autopolymerization of Pyrrole on UPD Cu-Modified Au Substrates. Figure 5 shows the SERS spectrum of the autopolymerized PPy film deposited on the UPD Cu-modified Au substrate. It is a typical Raman spectrum of polypyrrole deposited on metal substrates, as shown in the literature.[25,46] The peak shown at the higher frequency side of the double peaks of C−H in-plane deformation of PPy,[47] located at about 1055 and 1087 cm^{-1}, is characteristic of the oxidized PPy.[48] As described in the Experimental Section, the sample is free of pyrrole monomers in the SERS analysis. Thus, it certifies that

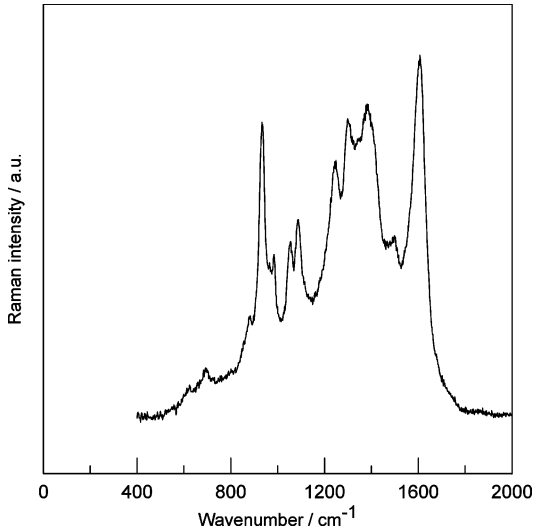

Figure 5. Raman spectrum of autopolymerized PPy on Au/UPD Cu substrate.

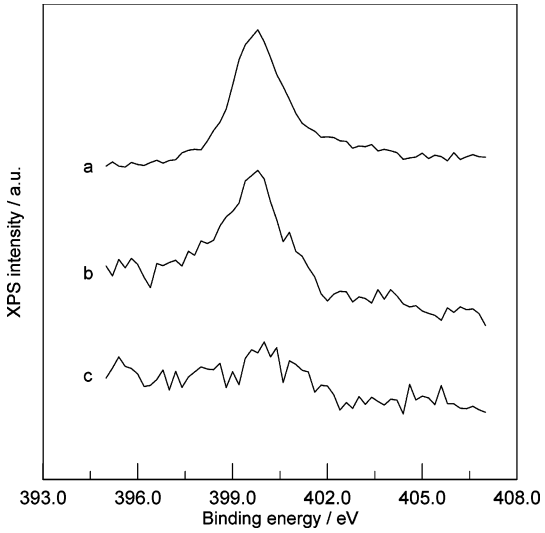

Figure 6. XPS N 1s core-level spectra of PPy layers on different substrates with and without sonicating treatments at various temperatures: (a) autopolymerized PPy on UPD Cu-modified Au substrate without sonicating treatment at room temperature of 22 °C; (b) autopolymerized PPy on UPD Cu-modified Au substrate with sonicating treatment for 30 min at elevated temperature of 70 °C; and (c) autopolymerized PPy on unmodified Au substrate with sonicating treatment for 30 min at elevated temperature of 70 °C for reference.

oxidized PPy can be produced, which is distinguishable from the known chemical or electrochemical method, on the UPD Cu-modified Au due to the special activity of the complexes. Furthermore, the peak located at 933.4 cm^{-1} is assigned to the C−H out-of-plane deformation of PPy.[49] It demonstrates a markedly enhanced intensity compared to that of PPy spectra generally shown in the literature.[25,46] According to surface selection rules of Raman and SERS, vibrations along the direction perpendicular to the surface should be more enhanced than those along the parallel direction.[50,51] Therefore, pyrrole monomers first orderly adsorb to the UPD Cu-modified Au substrate to form SAMs, followed by autopolymerization and further oxidation occurring on the substrate due to its special activity. The deposited PPy on the UPD Cu-modified Au substrate forms a densely packed monolayer parallel to the surface, which would reflect on the nucleation and growth mechanism of subsequent elecpolymerization of PPy, as will be discussed later.

The main problems of SAMs on unmodified substrates are the lack of stability of these films during long-term exposure to the atmosphere or to higher temperatures[9,10] and the easy exchange with a new thiol or related molecules. To examine the stability of autopolymerized PPy on the UPD Cu-modified Au substrate, desorption tests were performed in a sonicated bath at 70 °C for 30 min. Inspecting spectra a and b of Figure 6, before and after tests, respectively, it is found that the XPS N 1s core-level spectra of PPy are quite similar. This means that the deposited PPy on the UPD Cu-modified Au is stable. This may be ascribed to a stronger interaction between UPD Cu and PPy.[39] In contrast, the autopolymerized PPy on unmodified Au almost desorbs from the substrate after the test, as shown in Figure 6c.

Electropolymerization of Pyrrole on UPD Cu-Modified Au Substrates. As shown in the literature,[52,53] there are two kinds of nucleation, namely instantaneous and progressive, and two types of growth, such as two-dimensional (2D) and three-dimensional (3D). The number of nuclei in the instantaneous nucleation mechanism is constant, and they grow on their former positions on the bare substrate surface without the formation of new nuclei. Hence, the radii of the nuclei are larger and the surface morphology is rougher. In progressive nucleation, the nuclei grow not only on their former positions on the bare substrate surface but also on new nuclei which form smaller nuclei particles and the surface morphology is flatter. The current

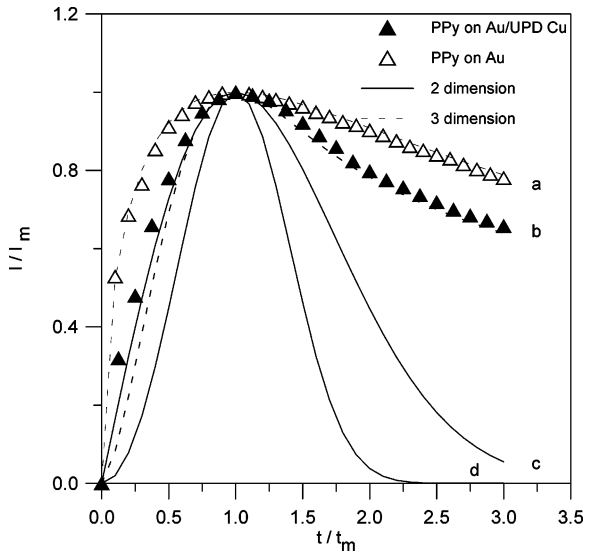

Figure 7. Dimensionless plots of $I-t$ curves for pyrrole polymerized on different Au substrates in 0.1 M pyrrole and 0.1 M $LiClO_4$ at 0.85 V vs Ag/AgCl, as compared with theoretical models for nucleation. Solid and open triangles represent PPy films electrodeposited on UPD Cu-modified Au and unmodified Au substrates, respectively. Curves a and b represent 3D instantaneous and progressive models (dashed lines), respectively. Curves c and d represent 2D instantaneous and progressive models (solid lines), respectively.

maximum (i_m) values for the electropolymerization of pyrrole on different electrodes, obtained from the chronoamperometric curves, are compared and fitted with the theoretical curves of 2D and 3D nucleation and growth obtained from those equations derived by Harrison and Thirsk[53] for the current−time relationship, as shown in Figure 7. It is clear that before and after nuclei overlapping (i_m), the nucleation and growth mechanisms for PPy electropolynerized on UPD Cu-modified Au and unmodified Au substrates are quite different. Before nuclei overlapping, the mechanisms obey the 2D instantaneous and 3D instantaneous nucleation and growth for the former and the latter, respectively. During the period of waiting for a steady OCP before starting

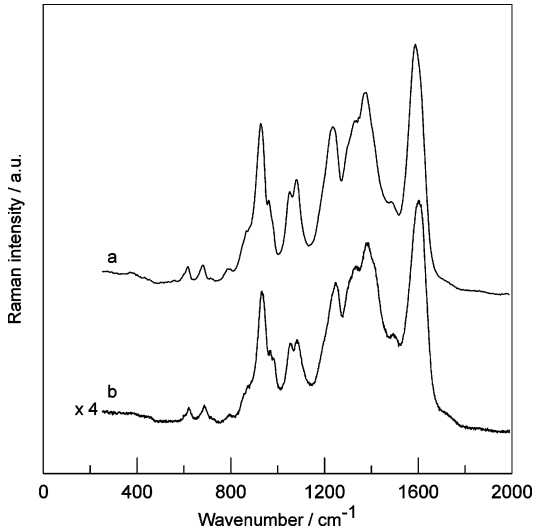

Figure 8. Raman spectra of PPy films electrodeposited on different substrates: (a) UPD Cu-modified Au substrate and (b) unmodified Au substrate; the intensity was magnified by 4-fold.

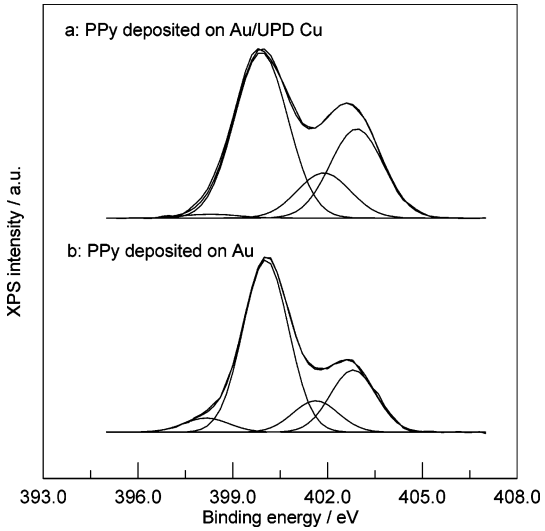

Figure 9. XPS N 1s core-level spectra of PPy films electrodeposited on different substrates: (a) UPD Cu-modified Au substrate and (b) unmodified Au substrate.

electropolymerization, an ordered layer of autopolymerized PPy, as discussed before, may have been formed on the UPD Cu-modified Au substrate. This autopolymerized PPy units can then serve as nucleation sites for the subsequent electrochemical growth of PPy. This 2D nucleation process results in a more compact layer, which is consistent with a flatter surface morphology obtained in the following 3D progressive nucleation process after nuclei overlapping for PPy deposited on the UPD Cu-modified Au substrate. This implies a more ordered nucleation process for the polymer formed on the modified electrode, since nucleation occurs at the sites of ordered autopolymerized PPy. This is also evidence of random nucleation followed by 3D growth on the unmodified substrate, as compared to a specific nucleation followed by an ordered growth for the modified electrode before nuclei overlapping. As shown in the literature,[54−57] a denser and more compact morphology would reflect on the enhancement of conductivity stability in the aging behavior of PPy films exposed to oxygen and water atmosphere, as shown later. Moreover, an encouraging phenomenon is that the conductivity of PPy deposited on the UPD Cu-modified Au substrate also can be enhanced, from 95.3 to 242 S cm^{-1}.

Figure 8 shows the Raman spectra of PPy films deposited on different gold substrates. Obviously, a PPy spectrum obtained on the UPD Cu-modified Au substrate exhibits both higher intensity (more than 4 times) and more excellent resolution. This increase in intensity is significant in comparison with the report of polyaniline chemically deposited on various rough metals by Baibarac et al.[58] This phenomenon of higher intensity and resolution can be explicated from the chemical effect of SERS, since charge transfer readily occurs between pyrrolylium nitrogen and UPD Cu. A similar report was also found in the literature.[59] Moreover, the oxidation degree[60] increases from 0.51 to 0.55, calculated from the double peaks of C−H in-plane deformation at 1052 and 1083 cm^{-1}, and the C═C backbone stretching[61] shifts from 1600 to 1590 cm^{-1} for PPy deposited on the UPD Cu-modified Au substrate. Both of them indicate that the conductivity of PPy is enhanced.

Figure 9 shows the XPS N 1s spectra of electropolymerized PPy deposited on UPD Cu-modified and unmodified gold substrates. With further deconvolution of N 1s spectra into four component peaks, the positively charged nitrogen ($-N^+H-$) species with the higher binding energy (BE) tail (BE > 401 eV) can be used to determine the oxidation level of PPy. This oxidation level is calculated from the ratio of the peak area of N^+(BE > 401 eV) to that of the total N 1s shown in the XPS spectrum.[62,63] The result shows that the oxidation level of PPy deposited on the modified electrode is 0.44, which is significantly higher in comparison with those of 0.33 for PPy deposited on the unmodified electrode and as-grown PPy, generally ranging from 0.25 to 0.33.[64] This higher oxidation level is reasonable for the corresponding enhanced conductivity obtained.[64]

To evaluate the effect of the modification of UPD Cu on the anti-aging ability of the electrodeposited PPy on it, stripped PPy films deposited on UPD Cu-modified Au and unmodified Au substrates were placed in an atmosphere of 50% RH and 20% (v/v) O_2 at 30 °C for 60 days. Detailed mechanisms of conductivity decay for PPy exposed to oxygen and water atmospheres were proposed in previous reports.[54,55] After aging, the conductivities decrease from 242 to 78.9 S cm^{-1} and from 95.3 to 19.4 S cm^{-1} for PPy films deposited on UPD Cu-modified Au and unmodified Au substrates, respectively. This reveals that electropolymerized PPy on the UPD Cu-modified Au substrate can depress its aging less of a decrease in conductivity.

Figure 10 demonstrates the conductivity decay as a function of aging time. The phenomenon of the increase in conductivity during the first 48 h was also reported in the previous study of PPy exposed to an atmosphere of 50% RH.[54] This increase in conductivity during this period can be ascribed to the solvation of the incorporated salt. The linear slope of the conductivity decay plot, except for the first 48 h, indicates that the process can be fitted to a first-order reaction kinetic in the range of 48−240 h, according to

$$\ln(\sigma/\sigma_o) = -kt \qquad (1)$$

where k is the degradation constant, and σ and σ_o are the conductivities of PPy films at time t in aging and as-grown PPy films, respectively. The calculated degradation rate constants are 5.15×10^{-3} and 7.44×10^{-3} h^{-1} for PPy films deposited on UPD Cu-modified Au and unmodified Au substrates, respectively. Moreover, after 60 days of testing, the conductivity decreases by 67.4% and by 79.6% for the former and the latter, respectively. Clearly, the PPy electropolymerized on the UPD Cu-modified Au becomes more stable.

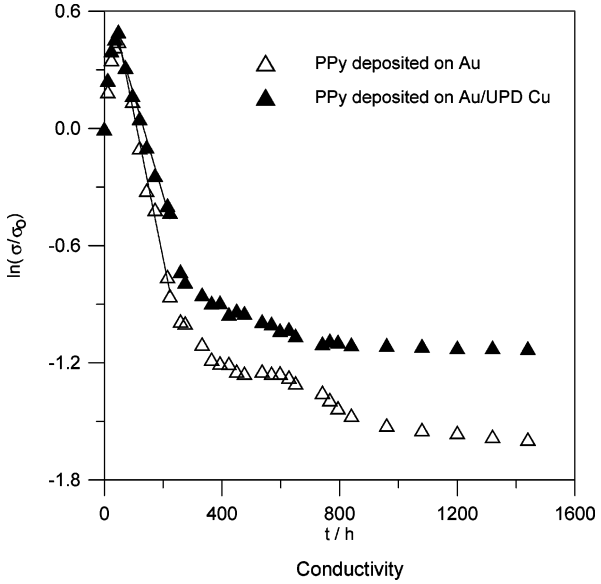

Figure 10. Variation of the electronic conductivity for PPy films electrodeposited on different substrates in 50% RH and 20% (v/v) O_2 at 30 °C for 60 days. Solid and open triangles represent UPD Cu-modified Au and unmodified Au substrates, respectively.

Conclusion

In this study, positively charged Cu, which is distinguished from the bulk Cu with zero charge, is successfully deposited on electrochemically roughened Au(111) for the first time by combining the techniques of UPD and roughening substrates by ORC treatments. Pyrrole monomers are found to adsorb onto the UPD Cu-modified Au to form orderly SAMs, and can be further autopolymerized due to the special activity of the nanocomplexes on the electrode. The stability of SAMs is significantly improved due to the presence of UPD Cu. Furthermore, electropolymerized PPy on the UPD Cu-modified Au demonstrates some distinguished properties. The conductivity is enhanced. Higher intensity and better resolution on SERS can be obtained. Moreover, the anti-aging ability in a 50% relative humility, 20% (v/v) O_2, and 30 °C atmosphere for 60 days is improved.

Acknowledgment. We thank the National Science Council of the Republic of China (NSC-91-2214-E-238-001) and Van Nung Institute of Technology for their financial support.

References and Notes

(1) Schondelmaier, D.; Cramm, S.; Klingeler, R.; Morenzin, J.; Zilkens, Ch.; Eberhardt, W. *Langmuir* **2002**, *18*, 6242.
(2) Huang, K.; Wan, M. *Chem. Mater*. **2002**, *14*, 3486.
(3) Vericat, C.; Lenicov, F. R.; Tanco, S.; Andreasen, G.; Vela, M. E.; Salvarezza, R. C.*J. Phys. Chem. B* **2002**, *106*, 9114.
(4) Lin, S. Y.; Tsai, T. K.; Lin, C. M.; Chen, C. H. *Langmuir* **2002**, *18*, 5473.
(5) Whelan, C. M.; Smyth, M. R.; Barnes, C. J. *Langmuir* **1999**, *15*, 116.
(6) Schoenfisch, M. H.; Pemberton, J. E. *J. Am. Chem. Soc*. **1998**, *120*, 4502.
(7) Lusk, A. T.; Jennings, G. K. *Langmuir* **2001**, *17*, 7830.
(8) Collard, D. M.; Sayre, C. N. *Synth. Met*. **1995**, *69*, 459.
(9) Carg, N.; Carrasquillo, M. E.; Lee, T. R. *Langmuir* **2002**, *18*, 2717.
(10) Valiokas, R.; Ostablom, M.; Svedhem, S.; Svensson, S. C. T.; Liedberg, B. *J. Phys. Chem. B* **2002**, *106*, 10401.
(11) Jennings, G. K.; Laibinis, P. E. *J. Am. Chem. Soc*. **1997**, *119*, 5208.
(12) Kim, T.; Crooks, R. M.; Tsen, M.; Sun, L. *J. Am. Chem. Soc*. **1995**, *117*, 3963.
(13) Wang, M. C.; Liao, J. D.; Weng, C. C.; Klauser, R.; Frey, S.; Zharnikov, M.; Grunze, M. *J. Phys. Chem. B* **2002**, *106*, 6220.
(14) Zamborini, F. P.; Campbell, J. K.; Crooks, R. M. *Langmuir* **1998**, *14*, 640.
(15) Lin, S. Y.; Chen, C. H.; Chan, Y. C.; Lin, C. M.; Chen, H. W. *J. Phys. Chem. B* **2001**, *105*, 4951.
(16) Zhang, M.; Wilde, C. P. *J. Electroanal. Chem*. **1995**, *390*, 59.
(17) Ozoemena, K.; Nyokong, T. *Electrochim. Acta* **2002**, *47*, 4035.
(18) Sonnichsen, C.; Franzl, T.; Wilk, T.; Von Plessen, G.; Feldmann, J. Wilson, O.; Mulvaney, P. *Phys. Rev. Lett.* **2002**, *88*, 774021.
(19) Sanchez-Cortes, S.; Domingo, C.; Garcia-Ramos, J. V. *Langmuir* **2001**, *17*, 1157.
(20) Hesse, E.; Creighton, J. A. *Langmuir* **1999**, *15*, 3545.
(21) Baibarac, M.; Lapkowski, M.; Pron, A.; Lefrant, S.; Baltog, I. *J. Raman Spectrosc.* **1998**, *29*, 825.
(22) Roy, D.; Furtak, T. E. *Chem. Phys. Lett.* **1986**, *124*, 299.
(23) Lefrant, S.; Baltog, I.; Baibarav, M.; Louarn, G.; Journet, C.; Bernier, P. *Synth. Met.* **1999**, *101*, 184.
(24) Lu, P.; Dong, J.; Toshima, N. *Langmuir* **1999**, *15*, 7980.
(25) Liu, Y. C. *Langmuir* **2002**, *18*, 174.
(26) Bukowska, J.; Jackowska, K. *Electrochim. Acta* **1990**, *35*, 315.
(27) Pemberton, J. E.; Guy, A. L.; Sobocinski, R. L.; Tuschel, D. D.; Cross, N. A. *Appl. Surf. Sci.* **1988**, *32*, 33.
(28) Gao, P. M.; Patterson, L.; Tadayyoni, M. A.; Weaver, M. J. *Langmuir* **1985**, *1*, 173.
(29) Taylor, C. E.; Pemberton, J. E.; Goodman, G. G.; Schoenfisch, M. H. *Appl. Spectrosc.* **1999**, *53*, 1212.
(30) Devine, T. M.; Furtak, T. E.; Macomber, S. H. *J. Electroanal. Chem.* **1984**, *164*, 299.
(31) Cai, W. B.; Ren, B.; Li, X. Q.; She, C. X.; Liu, F. M.; Cai, X. W.; Tian, Z. Q. *Surf. Sci.* **1998**, *406*, 9.
(32) Willicut, R. J.; McCarley, R. L. *J. Am. Chem. Soc.* **1994**, *116*, 10823.
(33) Willicut, R. J.; McCarley, R. L. *Anal. Chim. Acta* **1995**, *307*, 269.
(34) Rubinstein, I.; Rishpon, J.; Sabatani, E.; Redondo, A.; Gottesfeld, S. *J. Am. Chem. Soc.* **1990**, *112*, 6135.
(35) Sabatani, E.; Gafni, Y.; Rubinstein, I. *J. Phys. Chem.* **1995**, *99*, 12305.
(36) Kowalik, J.; Tolbert, L.; Ding, Y.; Bottomley, L.; Vogt, K.; Kohl, P. *Synth. Met.* **1993**, *55*, 1171.
(37) Willicut, R. J.; McCarley, R. L. *Langmuir* **1995**, *11*, 296.
(38) Wurm, D. B.; Brittain, S. T. Kim, Y. T. *Langmuir* **1996**, *12*, 3756.
(39) Liu, Y. C.; Hwang, B. J. *Thin Solid Films* **1999**, *339*, 233.
(40) Chang, R. K.; Laube, B. L. *CRC Crit. Rev. Solid State Mater. Sci.* **1984**, *12*, 1.
(41) Liu, Y. C. *Langmuir* **2002**, *18*, 9515.
(42) Liu, Y. C.; Jang, L. Y. *J. Phys. Chem. B* **2002**, *106*, 6748.
(43) Takami, S.; Jennings, G. K.; Laibinis, P. E. *Langmuir* **2001**, *17*, 441.
(44) Liu, Y. C.; Yang, K. H.; Ger, M. D. *Synth. Met.* **2002**, *126*, 337.
(45) Hammond, J. S.; Winograd, N. *J. Electroanal. Chem.* **1977**, *80*, 123.
(46) Wan, X.; Liu, X.; Xue, G.; Jiang, L.; Hao, J. *Polymer* **1999**, *40*, 4907.
(47) Furukawa, Y.; Tazawa, S.; Fujii, Y.; Harada, I. *Synth. Met.* **1988**, *24*, 329.
(48) Liu, Y. C.; Hwang, B. J. *Synth. Met.* **2000**, *113*, 203.
(49) Cheung, K. M.; Bloor, D.; Stevens, G. C. *Polymer* **1988**, *29*, 1709.
(50) Moskovits, M. *J. Chem. Phys.* **1982**, *77*, 4408.
(51) Gao, X. P.; Davies, J. P.; Weaver, M. J. *J. Phys. Chem.* **1990**, *94*, 6858.
(52) Hwang, B. J.; Santhanam, R.; Lin, Y. L. *J. Electrochem. Soc.* **2000**, *147*, 2252.
(53) Harrison, J. A.; Thirsk, H. R. *Electroanalytical Chemistry*; Marcel Dekker: New York, 1971; Vol. 5, p 67.
(54) Liu, Y. C.; Hwang, B. J. *J. Electroanal. Chem.* **2001**, *501*, 100.
(55) Liu, Y. C.; Hwang, B. J. *Thin Solid Films* **2000**, *360*, 1.
(56) Neoh, K.G.; Young, T. T.; Kang, E. T.; Tan, K. L. *J. Appl. Polym. Sci.* **1997**, *64*, 519.
(57) Dhanalakshmi, K.; Saraswathi, R.; Srinivasan, C. *Synth. Met.* **1996**, *82*, 237.
(58) Baibarac, M.; Cochet, M.; Lapkowski, M.; Mihut, L.; Lefrant, S.; Baltog, I. *Synth. Met.* **1998**, *96*, 63.
(59) Plays, B. J.; Bukowska, J.; Jackowska, K. *J. Electroanal. Chem.* **1997**, *428*, 19.
(60) Liu, Y. C.; Tsai, C. J. *Chem. Mater*. **2003**, *15*, 320.
(61) Tian, B.; Zerbi, G. *J. Chem. Phys.* **1990**, *92*, 3892.
(62) Kan, E. T.; Neoh, K. G.; Ong, Y. K.; Tan, K. L.; Tan, B. T. *Macromolecules* **1991**, *24*, 2822.
(63) Eaves, J. G.; Kopelove, A. B. *Polym. Commun.* **1987**, 28, 38.
(64) Skotheim, T. A. *Handbook of Conducting Polymers*; Marcel Dekker: New York, 1986; Chapter 8, p 275.